High responsivity GaS nanobelt metal-semiconductor-metal photodetector with Ni contact

Chun-Yi Lin[1], Chiu-Yen Wang [1*]
Department of Materials Science and Engineering, National Taiwan University of Science and Technology, Taiwan
(MOST 111-2221-E-011-107-MY2)

1. Experiment

Synthesis of GaS nanobelts

The precursor of gallium ingot 50 mg, sulfur powder 10 mg has been place at the bottom of the tube and maintain at 10^{-3} Torr and conducted the heat treatment to complete the reaction. A zirconia (ZrO_2) substrate, on which a 5 nm-thick Au film was deposited, was 10 cm away from the precursor. The whole system was heated to 900 °C in a single-zone furnace and kept for 1 hours. After reach to 900 °C, the GaS vaper will appear at the substrate position and form the GaS nanobelts.

2. Results and Discussions

3.1 SEM and EDS analysis of GaS nanobelts

Figure 1a and b depict low and high magnification scanning electron microscope (SEM) images, respectively. In these images, nanobelts are observed carrying small spherical catalyst particles at their tips, with diameters closely resembling the thickness of the nanobelt. The length of the nanobelts measures More than a hundred microns. The high magnification SEM image reveals that the structure grows into a belt-like form with a uniform thickness of approximately 100 nm. Energy-dispersive X-ray spectroscopy (EDS) analysis of the prepared sample indicates the presence of gallium and sulfur elements exclusively, with an atomic ratio close to 1. The precursor contributes to approximately 50% of gallium vapor, facilitating the formation of GaS nanobelts.

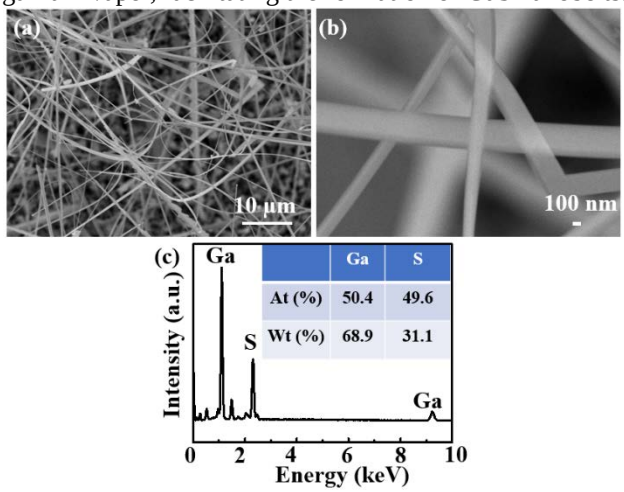

Figure 1. The (a) low and (b) high magnification SEM image of GaS nanobelts (c) The EDS analysis of as-grown GaS nanobelts show the ratio of Ga and S is close to 1

2.2 XRD and Raman analysis of GaS nanobelts

The XRD diffraction spectrum presented in Figure 2a reveals three main diffraction peaks located at 11.8°, 23.3°, and 35.1°, corresponding to the (002), (004), and (006) planes oriented to the hexagonal phase of β-GaS, with the space group P63/mmc. Figure 2b displays the Raman spectra results. The Raman shifts of the GaS nanobelt at room temperature are observed at E_{1g}^1, A_{1g}^1, E_{2g}^1, and A_{1g}^2, located at 76.7, 190.2, 294.6, and 361.3 cm^{-1}, respectively. It is notable that the first band vibration mode (A_{1g}^1 and A_{1g}^2) exhibits stronger intensity compared to the second vibration mode (E_{1g}^1 and E_{2g}^1). This discrepancy is attributed to the insufficient thickness of the nanobelt, making the detection of the second vibration mode (E_{1g}^1 and E_{2g}^1) more challenging.

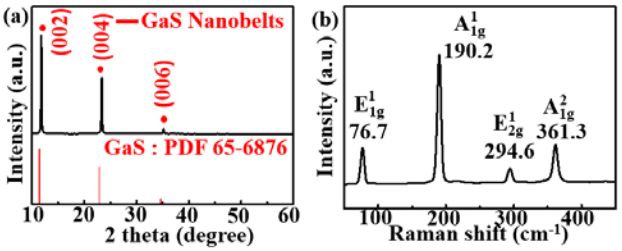

Figure 2 (a) XRD diffraction spectrum of GaS nanobelt and correspond with PDF-65-6876. (b) Raman spectroscopy of GaS nanobelts.

2.3 optoelectronic property of GaS nanobelts

Figure 3a shows the SEM image of the photodetector, show two Ni contacts was acted as the source and drain contact cover up the both side of the nanobelts. The laser radiation area is 0.303 μm^2. The device was exposure with three different wavelengths of laser, that is 405, 450 and 488 nm. As we know the bandgap of the GaS nanobelts is ~2.5 eV, there is no response when the laser wavelength is greater than 488 nm. Figure 3b-d shows the I-V characteristic with these three lasers in different laser power, respectively. The dark current is in several hundred fA at V = 1V. The photocurrent rising when the increase of the laser wavelength and show the maximum photocurrent at 405 nm light irradiation.

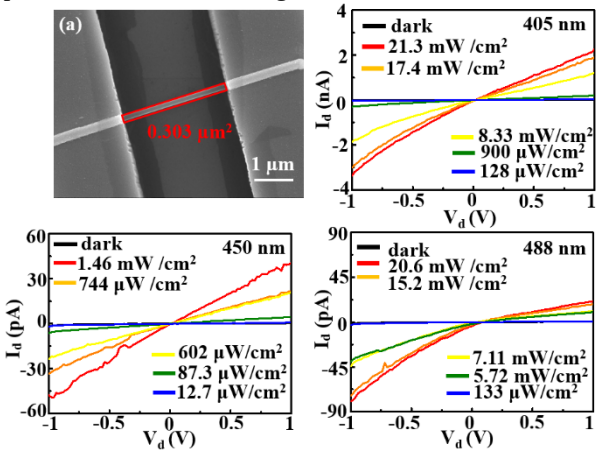

Figure 3 (a) SEM image of the optoelectronic device shows the illumination area is 0.303 μm^2. The I-V characteristic with (b) 405 nm (c) 450 nm and (d) 488 nm illumination light.

To further evaluate the performance of the photodetector, four crucial metrics are considered: light intensity-dependent photocurrents (I_{ph}), responsivity (R), external quantum efficiency (EQE), and detectivity (D*). Figures 4a-d illustrate the corresponding power density for each of these metrics. The maximum values of R, EQE, and D* are determined to be tens AW^{-1}, ~10^4 %, and ~10^{13} Jones, respectively, when exposed to a 405 nm laser with a power density of 128 μW/cm^2. It is noteworthy that all results exhibit a consistent trend: I_{ph} increases with rising power density, whereas R, EQE, and D* decrease with increasing power density. This trend is likely attributed to carrier recombination phenomena.

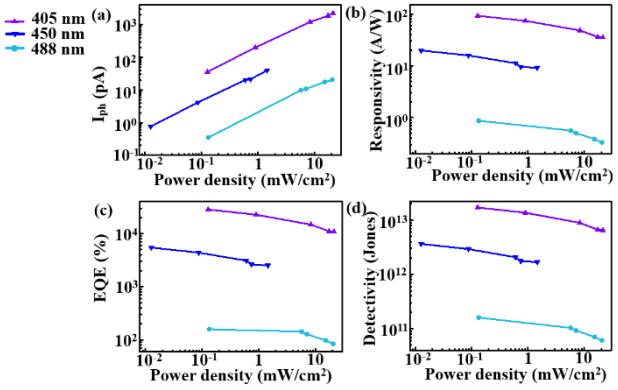

Figure 4 (a) I_{ph} (b) R (c) EQE (d) D* versus power density in 405, 450 and 488 illumination light.

Figure 5a displays the results of the I-T curve applied at the drain voltage of 1V with varying wavelengths. The switching on and off behavior demonstrates high stability and repeatability, indicating fast response times of the device. The rise and fall times, as depicted in Figures 5b and c, measure approximately 60 ms when exposed to a 405 nm wavelength. This response time is consistent with findings from previous literature, despite differences in contact, suggesting that the sensitive quality remains comparable to other studies. [1-2]

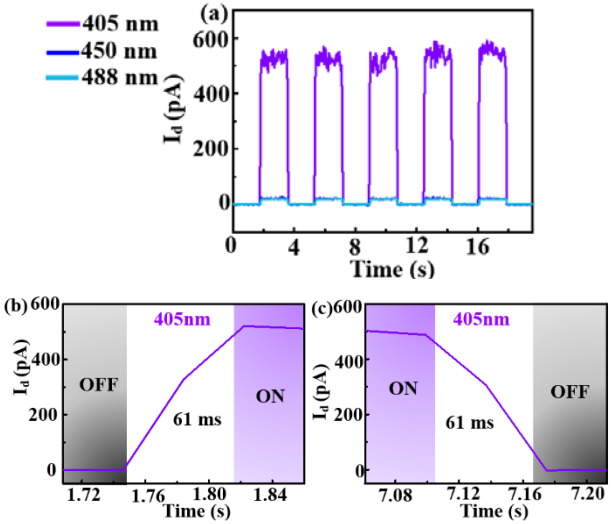

Figure 5 (a) I-T characteristic under incident light with different wavelengths. (b-c) The photoresponse rise time and fall time under 405 nm.

2.4 I-V characteristic after RTA

Figure 6a and c depict SEM images before and after rapid thermal annealing (RTA) at high temperature. The nanobelt is fully annealed in the latter image. Corresponding I-V curves are presented in Figures 6b and d, respectively. The device exhibits a significant increase in conductivity, up to 10^9 times. Furthermore, the nanobelts demonstrate metallic properties, which can be advantageous in forming $Ni_xGaS/GaS/Ni_xGaS$ heterostructure devices by controlling temperature and time parameters.

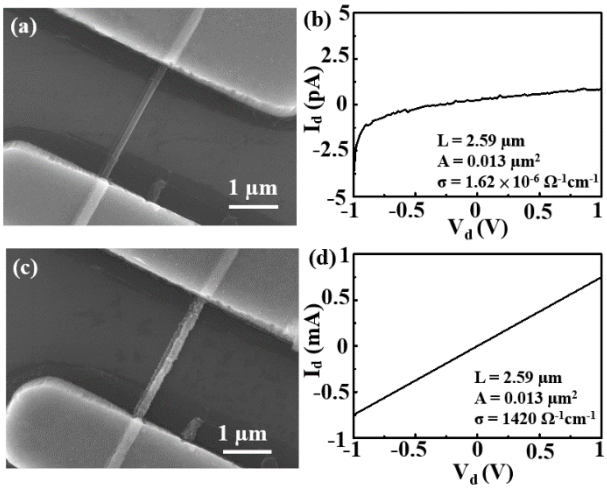

Figure 6 (a) SEM image and (b) I-V characteristic of the device before RTA and (c) SEM image and (d) I-V characteristic of the device after RTA.

3. Conclusion

In summary, GaS nanobelts with a 1:1 ratio were successfully synthesized via the VLS process, and their optoelectronic properties were systematically investigated. The GaS nanobelt photodetector demonstrates high responsivity under blue light emission, and the devices also exhibit fast response speeds. Additionally, after rapid thermal annealing (RTA), the properties of the nanobelts can be leveraged to fabricate heterostructure devices. Consequently, this semiconductor shows significant potential in high-responsivity photodetection, and this work may prove beneficial for electronic applications.

4. Ackownledgement

Chiu-Yen Wang acknowledges the financial support by the Ministry of Science and Technology through the grants of MOST 111-2221-E-011-107-MY2.

5. References

[1] Tongxin Chen, Yang Lu, Yuewen ShengGiangregorio, *et al* "Ultrathin All-2D Lateral Graphene/GaS/Graphene UV Photodetectors by Direct CVD Growth" ACS Application Material and interfaces 2019, 11, 48172-48178

[2] Yael Gutiérrez, Maria M. Giangregorio, Stefano Dicorato *et al* " Exploring the Thickness-Dependence of the Properties of Layered Gallium Sulfide" , Frontiers in Chemistry, 2021, 9, 781467